On characteristics of sheath damping near a dielectric wall with secondary electron emission*

Yu Da-Ren(于达仁)[a], Qing Shao-Wei(卿绍伟)[a)†],
Yan Guo-Jun(闫国军)[a], and Duan Ping(段 萍)[b]

[a] *School of Energy Science and Engineering, Harbin Institute of Technology, Harbin* 150001, *China*
[b] *School of Physics, Dalian Maritime University, Dalian* 116024, *China*

(Received 15 October 2010; revised manuscript received 21 December 2010)

A preliminary investigation is conducted to study the characteristics of sheath damping near a dielectric wall with secondary electron emission (SEE). Making use of the linear analysis of the sheath stability, we have found two major contributions to the sheath damping, one similar to the Landau damping in uniform plasmas and another determined by local electric field and electron density of the steady-state sheath. It indicates that in a classical sheath regime the damping in the sheath region monotonically increases towards the wall and decreases with the enhancement of SEE effect. In order to verify the theoretical analysis, sheath oscillation processes induced by an initial disturbance are simulated with a time-dependent one-dimensional (1D) sheath model. Numerical results obtained are consistent with the theoretical analysis qualitatively.

Keywords: plasma sheath, damping, electron electrostatic wave, secondary electron emission

PACS: 52.40.Kh, 52.35.Fp, 52.25.Dg **DOI:** 10.1088/1674-1056/20/6/065204

1. Introduction

Plasma sheath practically forms near solid surfaces bounded plasmas in the process of plasma-wall interaction. It is a long-standing problem in plasma physics yet to be fully understood. The problem of sheath formation at various plasma boundaries even recently still attracts much attention,[1−5] due to its particular importance in plasma science and technology. The structure of a steady state Debye layer near a dielectric wall was investigated by Morozov and Savelyev systematically.[6−8] In their studies, the secondary electron emission (SEE) of the dielectric wall determined wall potential and the distribution function of emitted electrons at the wall, as well as plasma behaviour in the sheath region. As related research and technology developed, sheath instabilities in plasma devices, such as Hall thrusters, were further studied due to its significant influence on the near-wall electron dynamics and thruster performance.[9−14] It was found that an important cause of the sheath instability was the high emission yield property of wall materials in the Hall thruster. It also suggested that the SEE of a dielectric wall might affect the stability parameters such as damping rate and frequency. Moreover, recent one-dimensional (1D) electron kinetic method[6,7] and two-dimensional (2D) particle-in-cell simulation[15] predicted that the sheath oscillation frequency was equal to electron plasma frequency and the sheath damping was zero as wall SEE was so strong that the sheath went into space charge saturated (SCS) regime. Thus, it is necessary to understand how the wall SEE affecting the sheath damping characteristics near a dielectric wall.

A possible mechanism is that the wall SEE affects the plasma oscillations via particle-wave interaction. In spite of the sheath being as thin as a few Debye lengths, the effective particle-wave interaction may still be also important due to the sharply varying electric field and electron density in the near-wall region. The wall SEE effect on the electric field and electron density can then act on the electron electrostatic wave in sheath region. In this paper, we try to clarify the sheath damping characteristics with SEE contribution near a dielectric wall. The paper is organized as follows. After the Introduction, we in Section 2 analyse the linear sheath stability. In Section 3, sheath oscillation processes induced by an initial disturbance are simulated with a time-dependent 1D sheath model

*Project supported by the National Natural Science Foundation for Distinguished Young Scholars (Grant No. 50925625), the National Natural Science Foundation of China (Grant Nos. 10975026 and 10875024), and the Scientific Research Foundation of the Higher Educational Institutions of Liaoning Education Bureau of China (Grant No. 2009A047).

†Corresponding author. E-mail: qshaowei@gmail.com

© 2011 Chinese Physical Society and IOP Publishing Ltd

combined with the SEE model of boron nitride (BN) ceramics. The damping rate in the sheath is then obtained with a curve fitting method based on a control theory of inertia and two-order oscillation systems. The numerical results are compared with the theoretical analysis. The conclusion is given in Section 4.

2. Theoretical analysis

A wave propagating in a uniform Vlasov–Poisson plasma with a Maxwellian distribution in the velocity space can be damped by the collisionless Landau damping mechanism.[16] For a nonuniform and nonlinear plasma sheath with a typical non-Maxwellian distribution, its damping mechanism and characteristic should vary significantly. In this section, applying linear instability analysis with the WKB approximation, we find that the sheath damping depends on the ratio of the electric field to the electron density in the steady-state sheath. Due to its effect on both parameters, we further indicate that the wall SEE can also significantly influence the sheath damping.

2.1. Linear analysis of sheath stability

We analyse first the linear sheath stability for the short-wavelength case. It is necessary to point out that, although the sheath is typically nonlinear and nonuniform, the linear theory is valid in qualitative and phenomenological analysis of sheath stability in the regime where the wavelength of the perturbation λ is far shorter than the sheath thickness L ($\lambda \ll L$). Therefore, in the WKB approximation, we can qualitatively analyse the sheath instability by a simplified 1D electron kinetic model as follows.

Assume that x is the coordinate across the sheath, the points $x = 0$ and $x = L$ are the plasma–sheath interface and the wall surface respectively. For a 1D steady-state sheath, the electron distribution function is $f_0(x, V)$, to give rise to the electron density $n_0(x) = \int_{-\infty}^{\infty} f_0(x, V)\,\mathrm{d}V$ and the electric field is $E_0(x)$. The sheath is also assumed unmagnetized. At the plasma–sheath boundary, the incident electron then obeys Maxwellian distribution, $f_0(0, V) = f_{\mathrm{Maxw}}(V)$, $V > 0$. For the short wavelength and high frequency electrostatic instability considered here, both magnetic and ion density perturbations are neglected.

Then the perturbations of the electric field, electron density and velocity distributions can be written as $E_1(t, x)$, $n_1 = \int_{-\infty}^{\infty} f_1(t, x, V)\,\mathrm{d}V$, and $f_1(t, x, V)$ respectively. The linear Vlasov–Poisson equations can then be obtained as

$$\frac{\partial f_1}{\partial t} + V\frac{\partial f_1}{\partial x} - \frac{e}{m_\mathrm{e}}E_1\frac{\partial f_0}{\partial V} - \frac{e}{m_\mathrm{e}}E_0\frac{\partial f_1}{\partial V} = 0,$$
$$\frac{\mathrm{d}E_1}{\mathrm{d}x} = -4\pi e n_1. \tag{1}$$

If the non-uniformity of the steady state is on the order of sheath thickness, $\mathrm{d}/\mathrm{d}x \sim 1/L$, the short wavelength electrostatic mode along x direction (normal to the wall) can be written under the WKB approximation, as $\{f_1,\ E_1\} = \{\hat{f}_1,\ \hat{E}_1\}\exp\left[\mathrm{i}\left(S(x) - \omega t\right)\right]$, where the wavenumber $k = \mathrm{d}S/\mathrm{d}x$ and $\hat{f}_1$, $\hat{E}_1$ are spatially slowly varied amplifications with $\mathrm{d}/\mathrm{d}x \ll k$. In the WKB approximation, the above equations then become

$$f_1 = \frac{\mathrm{i}\,eE_1}{m_\mathrm{e}}\frac{\partial f_0/\partial V}{\omega - kV} + \frac{\mathrm{i}\,e}{m_\mathrm{e}}E_0\frac{\partial f_1/\partial V}{\omega - kV},$$
$$\mathrm{i}\,kE_1 = -4\pi e n_1 = -4\pi e\int f_1\mathrm{d}V. \tag{2}$$

Substituting f_1 into Poisson equation, approximately we have

$$1 = \frac{\omega_0^2}{k^2}\int_{-\infty}^{+\infty}\frac{\partial\widehat{f}_0/\partial V}{V - \omega/k}\mathrm{d}V - \mathrm{i}\,\frac{eE_0}{km_\mathrm{e}}\int_{-\infty}^{+\infty}\frac{\partial\widehat{f}_1/\partial V}{V - \omega/k}\mathrm{d}V, \tag{3}$$

where, $\widehat{f}_0$ is the normalized distribution function of the steady state electron and $\widehat{f}_1 = f_1/n_1$ satisfies $\int_{-\infty}^{+\infty}\widehat{f}_1\mathrm{d}V = 1$, $\omega_0(x) = \sqrt{4\pi e^2 n_0(x)/m_\mathrm{e}}$ is the "local" electron frequency, with $\omega_0(0) = \omega_{\mathrm{pe}}$ being the plasma frequency at the plasma–sheath interface where the plasma density $n_{e0} = n_0(0)$.

The incident electrons ($f_0(x, V)$, $V > 0$) approximately obey Maxwellian distribution in the steady state sheath, though the relative low-energy incident electrons may be reflected by the electric field of the sheath. Thus, the first term on the right-hand side (RHS) of Eq. (3) is approximately the same as that in Landau's analysis for uniform plasmas.[16] As for the very low temperature sheath electron, the thermal term is small. Then, using Landau's integral, we can calculate the linear dispersion relation from Eq. (3) as

$$D^{\mathrm{L}}(\omega, k; x) \approx 1 - \frac{\omega_0^2}{\omega^2} - \pi\frac{eE_0}{km_\mathrm{e}}\left.\frac{\partial\widehat{f}_1}{\partial V}\right|_{\mathrm{V}=\omega/k} - \mathrm{i}\,\pi\frac{\omega_0^2}{k^2}\left.\frac{\partial\widehat{f}_0}{\partial V}\right|_{\mathrm{V}=\omega/k} + \mathrm{i}\,\frac{eE_0}{km_\mathrm{e}}\mathrm{P}\int_{-\infty}^{+\infty}\frac{\widehat{f}_1}{(V - \omega/k)^2}\mathrm{d}V, \tag{4}$$

where the operator P in the last term indicates the principal part of the integral. At the plasma–sheath

interface where $E_0 = 0$, the above dispersive relation becomes $\mathrm{Re}\,\omega = \omega_0 = \omega_{\mathrm{pe}}$ and

$$\mathrm{Im}\,\omega = \frac{\pi}{2}\frac{\omega_0^3}{k^2}\frac{\partial \widehat{f}_0}{\partial V}\bigg|_{\mathrm{V}=\omega/k} \ll \mathrm{Re}\,\omega,$$

the same as that of the Langmuir wave. For the electrostatic wave generated in the plasma and then transmitted into the sheath, its real frequency should be a constant during the propagation process in sheath region and approximately equal to the plasma frequency ω_{pe}. Taking into account of the imaginary part, we obtain

$$\omega \approx \omega_{\mathrm{pe}} + \mathrm{i}\left(\underbrace{\frac{\pi}{2}\frac{\omega_{\mathrm{pe}}^3}{k^2}\frac{\partial \widehat{f}_0}{\partial V}\bigg|_{\mathrm{V}=\omega/k}}_{\gamma_1} - \underbrace{\frac{E_0}{n_0}\frac{en_{e0}\omega_{\mathrm{pe}}}{2km_{\mathrm{e}}}\mathrm{P}\int_{-\infty}^{+\infty}\frac{\widehat{f}_1}{(V-\omega/k)^2}\mathrm{d}V}_{\gamma_2}\right). \tag{5}$$

It is shown that the damping in the sheath consists of two parts, namely γ_1 and γ_2, where γ_1 is similar to the Landau damping in uniform plasmas and γ_2 is determined by local electric field $E_0(x)$ and electron density $n_0(x)$ for a given $\widehat{f}_1$.

As for a perturbed distribution function $\widehat{f}_1$, the integral in Eq. (5) is positive, if $\widehat{f}_1 > 0$ near the resonance $V = \omega/k$. Then, the electrostatic sheath mode will be damped with $\mathrm{Im}\,\omega = \gamma_1 + \gamma_2 < 0$, for the Maxwellian steady state electrons. And the damping caused by the non-uniformity is relative to the ratio of the local electric field $E_0(x)$ to the electron density $n_0(x)$.

2.2. Effect of wall SEE on sheath damping characteristics

The dispersion relation (Eq. (5)) suggests that the sheath damping is determined by two steady-state sheath parameters, the electron density $n_0(x)$ and electric field $E_0(x)$. In general, the plasma sheath is formed near a solid surface due to the effect of ambipolar diffusion and the plasma-wall interaction. In order to shield the electric field generated by the charges accumulated on the wall surface, the sheath electric field $E_0(x)$ is generated by the charge separation

$$\frac{\mathrm{d}E_0(x)}{\mathrm{d}x} = 4\pi e\left[n_{\mathrm{i}}(x) - n_0(x)\right] = 4\pi Q(x),$$

where $n_{\mathrm{i}}(x)$ is the ion density and $Q(x)$ is the charge density. At plasma–sheath interface, $n_{\mathrm{i}}(0) = n_0(0) = n_{\mathrm{e0}}$, $E_0(0) = 0$ and $\mathrm{d}E_0/\mathrm{d}x = 0$.

In the classical sheath regime, E_0 increases monotonically toward the wall, because the net charge density in sheath region satisfies $Q = e(n_{\mathrm{i}} - n_0) > 0$. The secondary electrons emitted from the wall have a contribution to the electron density in sheath region, which results in charge separation weakening in the sheath, i.e., decreasing of Q. Thus, the sheath field $E_0(x)$ is reduced with the SEE effect enhancement, an effect also showed in many previous studies.[7,17–19]

However, as the total SEE yield on the wall is greater than a certain critical value, the sheath goes into SCS regime.[7,17] In this regime, $E_0(x)$ does not increase monotonically toward the wall but change the sign to $E_0(x) < 0$ in the near wall region. Therefore, the mode with the dispersion Eq. (5) may get unstable in SCS regime if $\gamma_2 > 0$ caused by $E_0(x) < 0$ overcomes the dimpling effect of γ_1 to lead to $\mathrm{Im}(\omega) = \gamma_1 + \gamma_2 > 0$. The instability caused by the high SEE yield of the wall has been verified by recent 1D electron kinetic method[6,7] and 2D particle-in-cell simulation[15] with the periodically oscillated sheath in SCS regime.

The above theoretical analysis shows qualitative predictions of the sheath damping characteristics. We are going to further verify them numerically.

3. Numerical verification

In this paper, we adopt a time-dependent 1D hybrid sheath model[7] of kinetic electrons and fluid ions to simulate the sheath oscillation process with initially nonuniform Maxwellian electron and a steady-state ion distribution. Then, in order to obtain sheath stability parameters such as damping rate and frequency, a control theory of inertia and two-order oscillation systems is used to fit the oscillation process of potential.

3.1. Numerical model

Assuming that the plasma sheath near a planar dielectric wall is collisionless and unmagnetized,

we describe the electron velocity distribution function $f_{\rm e}(t,x,V)$ by the Vlasov equation

$$\frac{\partial f_{\rm e}}{\partial t}+V\frac{\partial f_{\rm e}}{\partial x}-\frac{e}{m_{\rm e}}E\frac{\partial f_{\rm e}}{\partial V}=0, \tag{6}$$

where, x is the coordinate across the sheath with the plasma–sheath interface $x=0$ and the wall $x=L$; V is the x component of velocity, $m_{\rm e}$ is the electron mass, e is the element charge and $E=-\partial\Phi/\partial x$ is the electric field with the potential $\Phi(x,t)$ satisfying Poisson's equation

$$\frac{\partial^2\Phi}{\partial x^2}=-4\pi e\left(n_{\rm i}-n_{\rm e}\right). \tag{7}$$

The ion density $n_{\rm i}(x)$ and fluid velocity $U_i(x)$ are described by the hydrodynamic approximation

$$\begin{aligned}&\frac{\partial n_{\rm i}}{\partial t}+\frac{\partial\left(n_{\rm i}U_i\right)}{\partial x}=0,\\&\frac{\partial\left(n_{\rm i}U_i\right)}{\partial t}+\frac{\partial\left(n_{\rm i}U_i^2\right)}{\partial x}=\frac{en_{\rm i}}{m_i}E.\end{aligned} \tag{8}$$

At the left boundary ($x=0$), we assume that the potential is zero, $\Phi(0)=0$ and the electron entering the sheath with $V>0$ obeys a Maxwellian distribution

$$\begin{aligned}&f_{\rm e}(t,0,V)=n_{\rm e0}\left(\frac{m_{\rm e}}{2\pi T_{\rm e}}\right)^{1/2}\exp\left(-\frac{m_{\rm e}V^2}{2T_{\rm e}}\right),\\&V>0,\end{aligned} \tag{9}$$

where the parameters $n_{\rm e0}$ and $T_{\rm e}$ are respectively the density and temperature of the incident electrons at the sheath boundary.

As in Ref. [7], we assume the boundary condition of electric field at the wall is

$$E(L)=-2\pi\rho, \tag{10}$$

where ρ is the surface charge density and the possible surface conductivity of the dielectric is neglected.

Usually a certain SEE model is needed to calculate ρ and set the boundary condition for $f_{\rm e}$ at $x=L$. The characteristic quantities of the wall SEE consist of SEE yield $\sigma(\varepsilon_{\rm p})$ and SEE spectrum ${\rm d}\sigma/{\rm d}\varepsilon$, where $\varepsilon_{\rm p}$ and ε are the energy of incident and emitted electrons respectively. As for the SEE yield $\sigma(\varepsilon_{\rm p})$ of BN ceramic wall, the experimental data (shown in Fig. 1) indicates that $\sigma(\varepsilon_{\rm p})$ always bigger than 0.5 even when $\varepsilon_{\rm p}$ is very low due to the elastic reflection probability of incident electron. In general, the elastic reflection probability is high for dielectrics when $\varepsilon_{\rm p}$ is low and it rapidly increases below 30 eV up to a value of the order of 0.5 approximately at $\varepsilon_{\rm p}=5$ eV–10 eV.[20] In this paper, we used the SEE yield model of Ref. [15] to describe the SEE properties of BN ceramic wall. This SEE yield model contains the probability of four events that may occur as an electron with energy $\varepsilon_{\rm p}$ collides with the wall, given as follows:

absorbed by the wall

$$W_0(\varepsilon_{\rm p})=P_0\exp\left(-\varepsilon_{\rm p}^2/\alpha_0^2\right);$$

elastically reflected

$$W_{\rm r}(\varepsilon_{\rm p})=P_{\rm r}\exp\left(-\varepsilon_{\rm p}^2/\alpha_{\rm r}^2\right);$$

one true secondary electron emitted

$$W_1(\varepsilon_{\rm p})=1-W_0(\varepsilon_{\rm p})-W_{\rm r}(\varepsilon_{\rm p})-W_2(\varepsilon_{\rm p});$$

two true secondary electrons emitted

$$W_2(\varepsilon_{\rm p})=1-\exp\left(-\varepsilon_{\rm p}^2/\alpha_2^2\right).$$

Then the SEE yield is obtained as $\sigma(\varepsilon_{\rm p})=W_{\rm r}(\varepsilon_{\rm p})+W_1(\varepsilon_{\rm p})+2W_2(\varepsilon_{\rm p})$. The corresponding parameters used in our numerical computation are set as follows: $P_0=0.5$, $\alpha_0=43.5$, $P_{\rm r}=0.5$, $\alpha_{\rm r}=30$, $\alpha_2=127.9$. As shown in Fig. 1, one can find that the prediction of SEE yield model is approximately in accordance with the experimental data of BN ceramic wall. Furthermore, the SEE spectrum model ${\rm d}\sigma/{\rm d}\varepsilon$ used in this paper for a true electron emission event is the same as in Ref. [7].

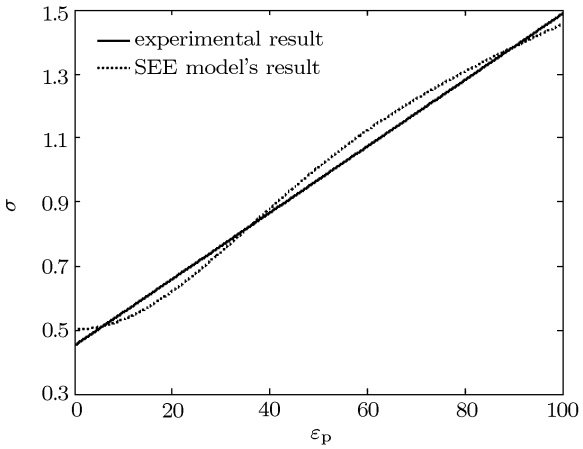


Fig. 1. Comparison of the SEE yield between SEE yield model and experimental data.[20]

In our computation model, the spatial length of sheath is $L=15\lambda_{\rm D}=15\left(T_{\rm e}/4\pi e^2n_{\rm e0}\right)^{1/2}$. At the plasma–sheath interface, the ion density is $n_{\rm i0}=n_{\rm e0}$ and the ion velocity is given by Bohm criterion $V_{\rm i0}=\left(T_{\rm e}/m_i\right)^{1/2}=0.01V_{\rm T0}$ with the assumption of the mass ratio of electron to ion $m_{\rm e}/m_i=10^{-4}$. Appropriate parameters are used to normalize the variables

in this sheath model, as n_{e0} for density, the electron thermal velocity V_{T0} for velocity, the Debye radius λ_D for length, $t_0 = \lambda_D/V_{T0} = \omega_{pe}^{-1}$ for time, T_e for energy and T_e/e for potential.

3.2. Initial conditions

Since we only consider electron oscillation in the sheath and the mass of electron is far less than that of ion, the ion in sheath is then considered as a background. In order to make the initial perturbation be sufficiently small, we assume that the steady state sheath initially with the electron in the sheath region obeys nonuniform Maxwellian distribution.

Removing the time differential terms in Eqs. (6) and (8), we can obtain a 1D steady-state sheath model combined with the SEE model of BN ceramics. With the method in Ref. [7], we solve the analytic distribution of the ion density in the sheath region at different electron temperatures (T_e = 5 eV–45 eV). The several typical density distributions of the electron and ion are shown in Fig. 2.

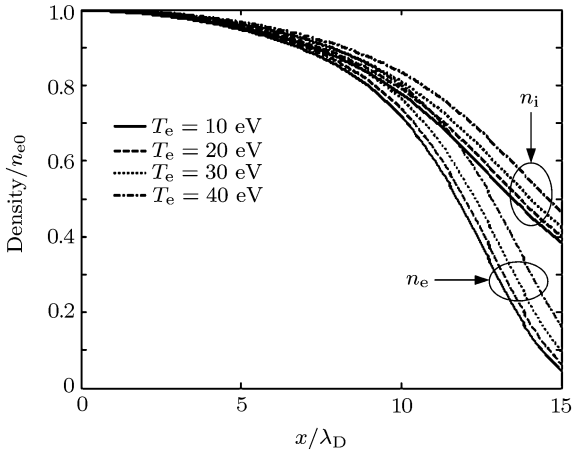


Fig. 2. Spatial profiles of n_e and n_i for different electron temperatures T_e.

3.3. Results of the damping in sheath region

For the sheath oscillation process simulation, we use a rectangular mesh for the x–V phase space with the computational domain of $0 \le x < L$, $|V| \le 4V_{T0}$. Let $N = 150$ and $M = 200$ designate the number of mesh points along x and V respectively. The time step is $\Delta t = 0.01\omega_{pe}^{-1}$. The kinetic equation was solved numerically by the time-splitting scheme combined with cubic spline interpolation method.[21] The electron temperature in the range of 5 eV–45 eV is considered in our calculation for the oscillation processes of the BN dielectric wall sheath relaxation to a steady state. All the calculation results predict a classical sheath structure,[7] and the main steady-state sheath parameters such as total SEE yield

$$\bar{\sigma} = \int_{-\infty}^{0} V f_e(L,V)\,\mathrm{d}V \Big/ \int_{0}^{\infty} V f_e(L,V)\,\mathrm{d}V$$

and the wall potential Φ_L increase with the plasma electron temperature T_e. The total SEE yield also can be obtained by using the formula

$$\bar{\sigma} = \int_{0}^{\infty} \sigma(\varepsilon_p) f_e(L,\varepsilon_p)\,\mathrm{d}\varepsilon_p \Big/ \int_{0}^{\infty} f_e(L,\varepsilon_p)\,\mathrm{d}\varepsilon_p,$$

where $\varepsilon_p = m_e V^2/2$. Using the SEE yield $\sigma(\varepsilon_p)$ of BN ceramic wall (shown in Fig. 1), we obtain that $\bar{\sigma} \ge \min\{\sigma(\varepsilon_p), \varepsilon_p \ge 0\} \approx 0.5$.

We then focus on the oscillation process of the potential to study the sheath damping characteristics. The potential oscillation at different positions of the sheath demonstrates a weak damping characteristic shown in Fig. 3. We can therefore consider the response of the sheath as it is stimulated by an initial disturbance to be a combination of an inertia system and a two-order oscillation system by referring to the related control theory of linear oscillation. Then the potential Φ can be fitted to a function as

$$\Phi(t) = a_0 + a_1 \mathrm{e}^{-\sigma_1 t} + \mathrm{e}^{-\sigma_2 t}\left[a_2 \cos\omega t + a_3 \sin\omega t\right], \quad (11)$$

where a_0, a_1, a_2, a_3, σ_1, and σ_2 are undetermined parameters and ω is the oscillation frequency.

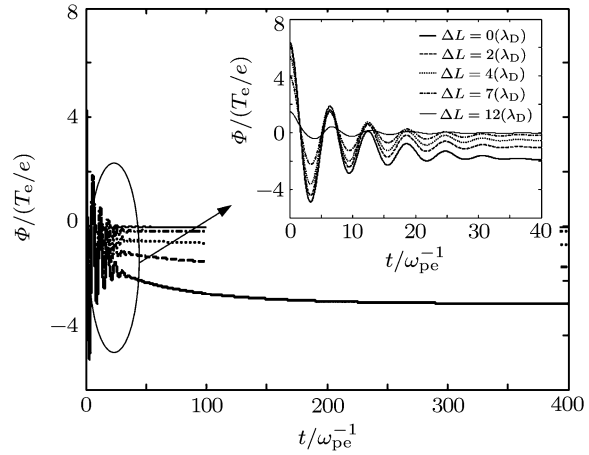


Fig. 3. Oscillation of the potential Φ at various positions, with T_e = 10 eV, and ΔL the distance from wall.

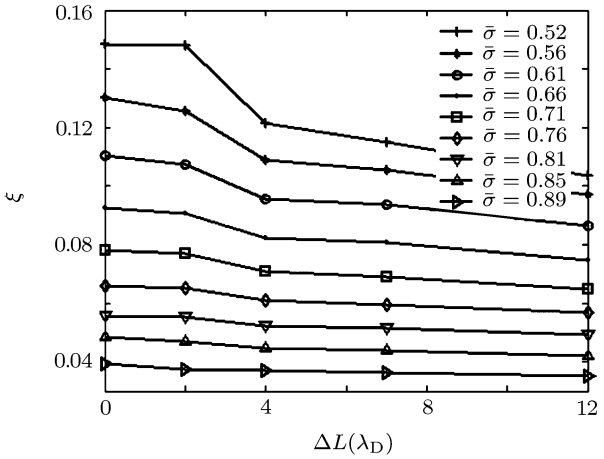


Fig. 4. Spatial distribution of the damping for different total SEE yields $\bar{\sigma}$.

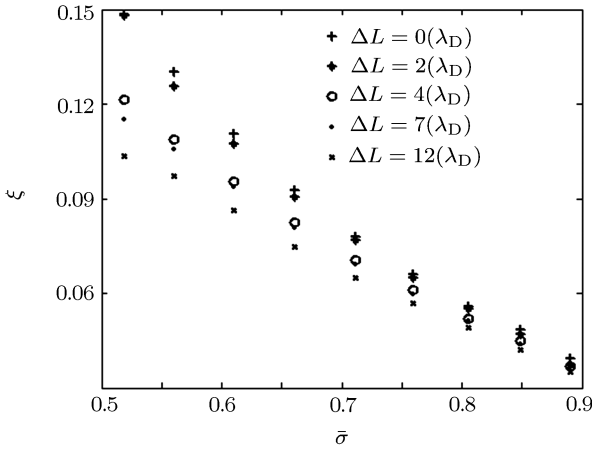


Fig. 5. The damping in different positions of the sheath versus the total SEE yield $\bar{\sigma}$ of steady-state sheath.

Using Eq. (11) to fit the oscillation process of potential Φ, we obtained the damping $\xi = \sigma_2/\sqrt{\sigma_2^2 + \omega^2}$ and the oscillation frequency ω of the sheath. All the fitting results indicate that the oscillation frequency ω is nearly equal to the plasma frequency $\omega_{\rm pe}$. The spatial profile of damping shown in Fig. 4 is in accordance with the theoretical analysis of the damping in sheath region that is monotonically increased toward the wall. Figure 5 shows that the damping ξ decreases linearly with the increases of total SEE yield $\bar{\sigma}$ approximately. It is qualitatively consistent with the theoretical analysis that the damping in sheath region decreases with the enhancement of SEE effect.

4. Conclusion

The damping characteristic of the sheath near a dielectric wall with the SEE effect has been studied theoretically by the linear theory under WKB approximation and numerically by a time-dependent 1D hybrid sheath model of kinetic electrons and fluid ions combined with the SEE model of BN ceramics. The theoretical analysis predicts that the damping in the sheath region should monotonically increase toward the wall and decrease with the enhancement of SEE effect. Also the spatial distribution of sheath damping and its variation versus the total SEE yield are qualitatively in accordance with the theoretical analysis. It is revealed that the nonuniform electric field and electron density in the sheath region can generate additional damping besides the Landau damping for the uniform plasma system.

Acknowledgements

We would like to thank Prof. Wang Xiao-Gang at State Key Lab of Nuclear Physics and Technology, School of Physics, Peking University, for providing careful revision of English and for his excellent analysis and discussion.

References

[1] Riemann K U 1991 *J. Phys.* D **24** 493
[2] Franklin R N 2004 *J. Phys.* D **37** 1342
[3] Riemann K U 2009 *Plasma Sources Sci. Technol.* **18** 014006
[4] Wang Z X, Liu J Y, Zhou X, Liu Y and Wang X G 2003 *Chin. Phys. Lett.* **20** 1537
[5] Wang D Z, Yu J and Gong Y 1996 *Chin. Phys. Lett.* **13** 117
[6] Morozov A I and Savelyev V V 2002 *Plasma Phys. Rep.* **28** 1017
[7] Morozov A I and Savelyev V V 2004 *Plasma Phys. Rep.* **30** 299
[8] Morozov A I and Savelyev V V 2007 *Plasma Phys. Rep.* **33** 20
[9] Sydorenko D, Kaganovich I, Raitses Y and Smolyakov A 2009 *Phys. Rev. Lett.* **103** 145004
[10] Sydorenko D, Smolyakov A, Kaganovich I and Raitses Y 2008 *Phys. Plasmas* **15** 053506
[11] Raitses Y, Staack D, Keidar M and Fisch N J 2005 *Phys. Plasmas* **12** 057104
[12] Taccogna F, Longo S, Capitelli M and Schneider R 2009 *Appl. Phys. Lett.* **94** 251502
[13] Yu D R, Li H and Wu Z W 2007 *Phys. Plasmas* **14** 064505
[14] Kirdyashev K P 1997 *Tech. Phys. Lett.* **23** 395
[15] Yu D R, Zhang F K, Liu H, Li H, Yan G J and Liu J Y 2008 *Phys. Plasmas* **15** 104501
[16] Landau L D 1949 *J. Phys.* **10** 25 (Moscow)
[17] Hobbs G D and Wesson J A 1967 *Plasma Phys.* **9** 85
[18] Li Y R, Ma J X, Zheng Y B and Zhang W G 2010 *Chin. Phys.* B **19** 085201
[19] Yu D R, Qing S W, Wang X G, Ding Y J and Duan P 2011 *Acta Phys. Sin.* **60** 025204 (in Chinese)
[20] Barral S, Makowski K, Peradzynski Z, Gascon N, Dudeck M 2003 *Phys. Plasmas* **10** 4137
[21] Cheng C Z and Knorr G 1976 *J. Comput. Phys.* **22** 330